IJARST

International Journal of Advanced Research in Science and Technology

https://doi.org/10.62226/ijarst20262748

ISSN 2319 – 1783 (Print)

ISSN 2320 – 1126 (Online)

An Experimental Digital Twin Framework for Online State Estimation and Feedback Control of an Induction Motor Drive

Darjon Dhamo*[1], Aida Spahiu[1], Denis Panxhi[1], Genci Sharko[1] and Nuri Rusta[2]

[1] Department of Automation, Faculty of Electrical Engineering, Polytechnic University of Tirana, Tirana, Albania

[2] Department of Electrical Engineering, Faculty of Electrical Engineering, Polytechnic University of Tirana, Tirana, Albania

** Corresponding author: darjon.dhamo@upt.al*

ARTICLE INFO

Article history:

Received	17 July 2026
Accepted	23 July 2026
Available online	31 July 2026

Keywords:

Digital Twin; Induction Motor; Extended Kalman Filter; Online State Estimation; Feedback Control.

Indexed in:

doi Crossref

INDEX COPERNICUS INTERNATIONAL

Google scholar

and in major libraries

ABSTRACT

The implementation of a Digital Twin for electric drives requires the combination of measurement synchronization, a realistic virtual model, state estimation, and feedback to the physical system. This paper describes an experimental realization of a Digital Twin for an induction motor fed by a variable frequency drive. The measured quantities, the three-line voltages, three-line currents, and encoder counts, are acquired on a PC using MATLAB. The measured signals are converted into physical units, despiked using causal robust filtering, transformed into the stationary reference frame, and synchronized across different sampling rates. Electrical and mechanical measurements are processed and synchronized at rates suitable for online Extended Kalman Filter (EKF) operation. The model consists of six states and works in the stationary reference frame, calculating the stator current, rotor flux components, rotor speed, and the load torque. A supervisory algorithm evaluates the estimated operating conditions and updates the inverter compensation parameter. The command is transmitted through Modbus TCP to adjust the inverter V/f characteristic within predefined limits. Experiments at 40 Hz and 45 Hz show that the estimator remains synchronized with the physical drive. The Digital Twin feedback improves rotor flux retention and maintains stable motor operation under changing operating conditions. These results show that the proposed system can perform the complete Digital Twin process, from online measurement and state estimation to the application of feedback commands to the induction motor drive.

1. Introduction

Digital Twins are increasingly used to establish a dynamic connection between physical assets and their corresponding virtual representations, which are continuously updated using measured data from the physical system. The virtual representation is continuously updated using measurement data collected from the physical system. When the operating conditions of the physical system change, the new data are transferred to the virtual model, allowing it to reflect these changes and provide a current description of the system's behavior. However, the term Digital Twin should be used carefully, because its correct definition depends on the presence and direction of automatic data exchange between the physical system and its virtual representation [1]. A digital model has no automatic data connection with the physical asset, a Digital Shadow receives data automatically from the asset without sending actions back, and a Digital Twin enables bidirectional interaction in which data update the virtual model and the resulting information can modify the operation of the physical system [1]–[5].

This difference is important in electric drive systems, because an online motor model or state observer cannot be considered a complete Digital Twin unless it is integrated with both the data acquisition system and the feedback control loop.

Induction motors supplied by power converters are nonlinear systems whose behavior depends on their electrical and mechanical parameters. The measured voltages and currents are affected by converter switching disturbances, while quantities such as rotor flux, electromagnetic torque, and load torque cannot normally be measured using standard sensors. Online estimation is therefore necessary to monitor the condition of the system and to support control or maintenance actions based on its current operating state. The Extended Kalman Filter (EKF) is suitable for this application because it combines a nonlinear model of the induction motor with measured current and speed data. It continuously corrects the predicted states by considering the uncertainty associated with both the model and the measurements [6]–[9]. Reliable real time execution also requires (i) signal processing methods that use only present and past measurements, (ii) accurate synchronization of measurements collected at different sampling rates, (iii) robust treatment of abnormal differences between predicted and measured values, and (iv) predefined limits on control commands to ensure safe operation of the physical system.

Previous studies have developed accurate induction motor models, experimental methods for identifying motor parameters, and EKF observers [8]–[14]. However, most studies address these elements separately and do not demonstrate a complete experimental workflow from raw measurement acquisition and processing to online state estimation and automatic feedback generation. Previous studies rarely document the combined use of causal signal processing, synchronization of measurements acquired at different rates, supervisory decision making, and inverter communication within a single bidirectional Digital Twin framework. Moreover, relatively few studies report soft real-time implementation on a standard PC rather than on dedicated real-time hardware. This study addresses these gaps by implementing and validating a complete Digital Twin framework that connects measured motor data with EKF state estimation, supervisory evaluation, and feedback to the inverter through Modbus TCP protocol.

The main contributions of this study are: (i) a complete workflow that transfers data from the physical motor drive to the virtual model by collecting and processing three phase voltages, currents, and encoder counts using only the measurements available at each time step; (ii) a six state EKF that operates at fixed time intervals and (iii) a feedback application that uses the estimated rotor flux and load torque to calculate gradual adjustments to an inverter parameter that modifies the V/f characteristic, with the commands transmitted through Modbus TCP.

The remainder of this paper is organized as follows. Section 2 describes the proposed methodology, including the experimental platform, data acquisition and signal processing procedures, the six state EKF, and the application layer that generates and sends feedback control commands to the inverter. Section 3 presents experimental results, including the online state estimation performance, the effect of feedback control, and the practical limitations of the implementation. Finally, Section 4 summarizes the main findings and identifies possible directions for future work.

2. Methodology

The methodology was organized into seven consecutive steps that connect the physical induction motor drive with its virtual representation and feedback application. It begins by operating the physical induction motor drive under defined conditions and measuring its electrical and mechanical variables. The acquired data are then transferred to a computer, processed, synchronized, and supplied to a dynamic motor model. An EKF combines model predictions with the available measurements to estimate quantities that cannot be obtained directly from standard sensors. Finally, selected estimated quantities are evaluated by a supervisory application that generates a control command restricted to predefined operating limits.

The main purpose of this procedure is to establish a complete experimental path from the physical drive to the virtual model and back to the physical system. Table 1 summarizes the role and output of each methodological step.

Table 1. Summary of the methodological steps.

Step	Main activity	Resulting output
Step 1	Operate the motor drive	Test conditions
Step 2	Measure voltage, current, and speed	Raw measurements
Step 3	Collect and transfer data	Digital data
Step 4	Process and synchronize signals	Prepared signals
Step 5	Run the virtual motor model	Predicted states
Step 6	Estimate motor states using the EKF	Estimated states
Step 7	Evaluate states and send feedback	Inverter command

2.1 Step 1: Operation of the Physical Induction Motor Drive

The first step consists of operating the physical induction motor drive under selected electrical and mechanical conditions. As shown in Fig 1, the experimental platform consists of a variable frequency drive supplying a three-phase induction motor. The motor shaft is mechanically connected through a belt and pulley transmission to an automotive alternator, which is connected to a battery and an adjustable electrical load.

This configuration provides an adjustable mechanical load and enables the motor to be tested at different inverter reference frequencies. The alternator and rheostat vary the mechanical torque applied to the motor, while the inverter controls the supply frequency and voltage.

Fig 1_Experimental platform of the electric drive and measurement system

The main technical specifications of the physical drive, mechanical load, measurement system, data acquisition equipment, and communication interface are summarized in Table 2.

Table 2. Technical data of the experimental, measurement, and acquisition system.

Subsystem	Component	Technical data
Physical drive	Variable frequency drive	Mitsubishi FR-D720S-014SC-EC; 0.2 kW; 1.4 A; 0.2–400 Hz
Physical drive	Induction motor	130 W; 220/380 V Δ/Y; 50 Hz; 2900 rpm
Mechanical load	Transmission and alternator	Belt and pulley drive; alternator 14 V, 95 A
Mechanical load	Battery and rheostat	12 V, 62 Ah battery; 7.5 Ω, 10 A adjustable rheostat
Measurement	Line voltages	Three channels; voltage dividers with galvanic isolation
Measurement	Line currents	Three channels; 0.1 Ω shunts with AMC1300 isolation
Measurement	Rotor speed	Incremental encoder; 1000 pulses/revolution
Data acquisition	DAQ hardware	NI PCI-6251 with BNC-2120; differential analog inputs and counter input
Data acquisition	Sampling and software	10 kHz analog acquisition; MATLAB on a standard PC
Communication	Inverter feedback	Modbus TCP

During each experiment, the drive is initially operated under predefined reference conditions. The motor operating frequency or mechanical load is changed to evaluate how the physical system responds and how accurately the estimator tracks the new operating condition. The resulting feedback command from the application layer is then applied to evaluate its effect on motor performance.

2.2 Step 2: Measurement of Electrical and Mechanical Quantities

Three-line voltages and three-line currents are measured at the output of the inverter to describe the electrical operating condition of the induction motor. Rotor motion is measured using an incremental encoder mounted on the motor shaft, with a resolution of 1000 pulses per revolution. The voltage measurement channels use high resistance dividers to reduce the inverter output voltage to a level compatible with the acquisition system, while the current channels use 0.1 Ω shunt resistors to generate proportional measurement signals. AMC1300 isolation amplifiers are used in both the voltage and current measurement circuits to provide galvanic separation between the power circuit and the data acquisition equipment. Rotor speed is calculated from the encoder pulse count over a 50 ms observation window, which is updated every 2 ms. Because the electrical signals are sampled more frequently than the speed measurement is updated, the electrical and speed measurements are synchronized before being supplied to the state estimator.

2.3 Step 3: Data Acquisition and Transfer to the Computer

The conditioned voltage and current signals are connected to the NI PCI 6251 data acquisition board through the BNC 2120 interface. The six analog channels are sampled in differential mode at 10 kHz, while the encoder pulses are recorded through a dedicated counter input. The acquisition system converts the measured signals into digital data and transfers them to a standard PC for further processing.

MATLAB manages the complete online workflow, including signal processing and synchronization, numerical execution of the motor model, state estimation, data recording, and Modbus TCP communication with the inverter. The implementation operates in soft real time, meaning that the measurements are processed and the estimated states are updated while the experiment is running, although execution at precisely fixed time intervals cannot be ensured.

2.4 Step 4: Signal Processing and Synchronization

The fourth step prepares the measured signals for use by the virtual motor model and the state estimator. Measurements obtained from the converter supplied motor contain switching disturbances, isolated abnormal samples, and scaling effects introduced by the measurement circuits. Therefore, the raw data acquisition values are first converted into volts and amperes using experimentally determined calibration factors:

$$v[n] = C_v \cdot v_{DAQ}[n], \quad i[n] = C_i \cdot i_{DAQ}[n] \tag{1}$$

where C_v and C_i are the voltage and current calibration factors respectively.

A causal cleaning method is then applied separately to the voltage and current signals. The method uses only the current sample and previously acquired measurements, making it suitable for online operation. For each voltage channel, an abnormal sample is replaced by the most recent valid value according to:

$$\tilde{v}[n] = \begin{cases} v[n], & |v[n] - m_v| \leq K_v(1.4826 \cdot MAD_v) \\ \tilde{v}[n-1], & |v[n] - m_v| > K_v(1.4826 \cdot MAD_v) \end{cases} \tag{2}$$

where m_v and MAD_v denote the median and median absolute deviation of the voltage signal. For each current channel, the change between consecutive samples is calculated as:

$$d_i[n] = i[n] - i[n-1] \tag{3}$$

and unusually large variations are rejected using

$$\tilde{\iota}[n] = \begin{cases} i[n], & |d_i[n] - m_{d_i}| \le K_i \cdot s_{d_i} \\ \tilde{\iota}[n-1], & |d_i[n] - m_{d_i}| > K_i \cdot s_{d_i} \end{cases} \quad (4)$$

with

$$s_{d_i} = \max(1.4826 \cdot MAD_{d_i}, s_{min}) \quad (5)$$

Where K_v and K_i are predefined rejection thresholds and s_{min} prevents an unrealistically small current variation scale. This approach suppresses isolated converter disturbances while preserving the main waveform of each signal.

The processed electrical samples are subsequently averaged in groups of three before each estimator update:

$$\bar{x}[k] = \frac{1}{N_b} \sum_{r=0}^{N_b-1} \tilde{x}[kN_b - r], \qquad N_b = 3 \quad (6)$$

Since the analog acquisition rate is 10 kHz, this averaging produces an effective estimator update of approximately 3.33 kHz. Rotor speed is calculated from the encoder count increment over a measurement window T_w:

$$n(t_k) = \frac{60 \cdot \Delta N_k}{PPR \cdot T_w} \quad (7)$$

where ΔN_k is the number of encoder pulses recorded during the window, PPR $= 1000$ pulses per revolution, and $T_w = 0.05$ s. The speed value is updated every 0.002 s, and the most recent valid value is retained between consecutive updates.

Because the induction motor stator is delta connected, the measured line currents are converted into stator phase currents before applying the coordinate transformation:

$$\begin{bmatrix} i_a \\ i_b \\ i_c \end{bmatrix} = \frac{1}{3} \begin{bmatrix} 1 & -1 & 0 \\ 0 & 1 & -1 \\ -1 & 0 & 1 \end{bmatrix} \begin{bmatrix} i_1 \\ i_2 \\ i_3 \end{bmatrix} \quad (8)$$

The mean value is then removed from each three-phase set:

$$\bar{x} = \frac{x_a + x_b + x_c}{3} \quad (9)$$

$$x_a^* = x_a - \bar{x}, \quad x_b^* = x_b - \bar{x}, \quad x_c^* = x_c - \bar{x} \quad (10)$$

Finally, the voltage and current quantities are transformed into the stationary $\alpha\beta$ reference frame using the Clarke transformation:

$$\begin{bmatrix} x_\alpha \\ x_\beta \end{bmatrix} = \frac{2}{3} \begin{bmatrix} 1 & -\frac{1}{2} & -\frac{1}{2} \\ 0 & \frac{\sqrt{3}}{2} & -\frac{\sqrt{3}}{2} \end{bmatrix} \begin{bmatrix} x_a^* \\ x_b^* \\ x_c^* \end{bmatrix} \quad (11)$$

The transformed voltage components are supplied as inputs to the dynamic motor model, while the transformed current components and synchronized speed values are used in the state correction stage. At the end of this step, the estimator receives calibrated, cleaned, averaged, transformed, and time synchronized measurements.

2.5 Step 5: Execution of the Virtual Motor Model

The fifth step uses a nonlinear mathematical model to represent the dynamic behavior of the induction motor. The model is formulated in the stationary $\alpha\beta$ reference frame and receives the processed stator voltage components from Step 4 as inputs. It describes the interaction between stator currents, rotor flux, mechanical speed, electromagnetic torque, and load torque.

The state and input vectors are defined as:

$$x = [i_{s\alpha} \quad i_{s\beta} \quad \Psi_{r\alpha} \quad \Psi_{r\beta} \quad \omega_m \quad T_L]^T \quad (12)$$
$$u = [u_{s\alpha} \quad u_{s\beta}]^T$$

The state vector contains the two stator current components, the two rotor flux components, the mechanical angular speed, and the load torque. The input vector contains the stator voltage components expressed in the stationary reference frame. The leakage factor, rotor time constant, and current damping coefficient are defined as

$$\sigma = 1 - \frac{L_m^2}{L_s L_r}, \qquad T_r = \frac{L_r}{R_r}, \qquad \gamma = \frac{R_s}{\sigma L_s} + \frac{1-\sigma}{\sigma T_r} \quad (13)$$

Table 3 Parameters of the Nonlinear Induction Motor Model

Parameter	**Description**
R_s, R_r	Stator and rotor resistances
L_s, L_r, L_m,	Stator, rotor, and magnetizing inductances
σ, T_r	Leakage factor and rotor time constant
J, B	Inertia and viscous friction coefficient
p	Number of pole pairs
T_L	Mechanical load torque

The stator current equations account for the applied stator voltages, resistive voltage drops, rotor flux contributions, and electromechanical coupling caused by rotor motion:

$$\frac{di_{s\alpha}}{dt} = -\gamma i_{s\alpha} + \frac{L_m}{\sigma L_s L_r T_r}\Psi_{r\alpha} + \frac{pL_m}{\sigma L_s L_r}\omega_m \Psi_{r\beta} + \frac{u_{s\alpha}}{\sigma L_s} \quad (14)$$

$$\frac{di_{s\beta}}{dt} = -\gamma i_{s\beta} + \frac{L_m}{\sigma L_s L_r T_r}\Psi_{r\beta} - \frac{pL_m}{\sigma L_s L_r}\omega_m \Psi_{r\alpha} + \frac{u_{s\beta}}{\sigma L_s} \quad (15)$$

The rotor flux components are determined from the stator currents, rotor time constant, and mechanical speed. The coupling terms describe the rotation of the rotor flux vector in the stationary reference frame:

$$\frac{d\Psi_{r\alpha}}{dt} = -\frac{\Psi_{r\alpha}}{T_r} + \frac{L_m}{T_r} i_{s\alpha} - p\omega_m \Psi_{r\beta} \quad (16)$$

$$\frac{d\Psi_{r\beta}}{dt} = -\frac{\Psi_{r\beta}}{T_r} + \frac{L_m}{T_r} i_{s\beta} + p\omega_m \Psi_{r\alpha} \quad (17)$$

The electromagnetic torque is calculated from the coupling between the rotor flux and stator current components:

$$T_e = \frac{3}{2} p \frac{L_m}{L_r} (\Psi_{r\alpha} i_{s\beta} - \Psi_{r\beta} i_{s\alpha}) \tag{18}$$

The mechanical equation relates the electromagnetic torque to rotor acceleration, viscous friction, and load torque:

$$J \frac{d\omega_m}{dt} = T_e - B\omega_m - T_L, \qquad \frac{dT_L}{dt} = 0 \tag{19}$$

The electrical and mechanical parameters are obtained from independent experimental identification tests and remain constant during the reported experiments. At each calculation interval, the virtual model predicts the evolution of the motor states, including quantities that are not measured directly, such as rotor flux, electromagnetic torque, and load torque. Measurement noise, parameter uncertainty, and unmodelled effects can cause the open loop model to gradually deviate from the physical motor drive. Therefore, the EKF described in Step 6 is used to correct the model predictions.

2.6 Step 6: Online State Estimation

The sixth step applies an EKF to combine the predictions of the six-state nonlinear motor model with the measured stator currents and encoder speed. At each calculation interval, the estimator first predicts the motor states and then corrects them using the available measurements. This process reduces the deviation between the virtual model and the physical drive.

During the prediction stage, the nonlinear motor model is integrated using a second order Runge Kutta method:

$$\hat{x}_k^- = f_{RK2}(\hat{x}_{k-1}^+, u_k, \Delta t) \tag{20}$$

where $\hat{x}_k^-$ is the predicted state vector, u_k contains the stator voltage components, and Δt is the estimator time interval. The predicted covariance matrix is calculated as

$$F_k \approx I + \Delta t A_k, \qquad P_k^- = F_k P_{k-1} F_k^T + Q_k \tag{21}$$

where A_k is the Jacobian matrix of the nonlinear motor model, F_k is the state transition matrix, P_k^- represents the predicted estimation uncertainty, and Q_k is the process noise covariance matrix.

During the correction stage, the measurement residual represents the difference between the measured output and the output predicted by the model:

$$r_k = y_k - h(\hat{x}_k^-) \tag{22}$$

The Kalman gain is then calculated from

$$K_k = P_k^- H_k^T (H_k P_k^- H_k^T + R_k)^{-1} \tag{23}$$

and the corrected state estimate is obtained as

$$\hat{x}_k = \hat{x}_k^- + K_k r_k, \qquad P_k = (I - K_k H_k) P_k^- \tag{24}$$

where H_k is the measurement matrix and R_k is the measurement noise covariance matrix.

The stator current components are included in every correction step because they are available at the electrical acquisition rate. Encoder speed is included whenever a new valid value becomes available. Therefore, the estimator combines fast current measurements with mechanical information obtained at a slower rate. The six estimated states are the two stator current components, the two rotor flux components, mechanical angular speed, and load torque. Including load torque as a state allows variations in mechanical demand to be followed without using a dedicated torque sensor.

To maintain stable online operation, the estimator is activated only after motor operation has been detected from the measured current. Large differences between predicted and measured values are limited or rejected to prevent excessive state corrections. Covariance limits are also applied to maintain numerical stability, while the estimated speed, rotor flux, and load torque are restricted to physically meaningful ranges.

The main outputs of this step are the corrected estimates of stator current, rotor flux, mechanical speed, electromagnetic torque, and load torque. These quantities describe the current operating condition of the motor and are transferred to the supervisory application in Step 7.

2.7 Step 7: Supervisory Evaluation and Feedback Command

The seventh step evaluates the estimated operating condition of the induction motor and determines whether a corrective command should be transmitted to the inverter. The supervisory application receives the estimated rotor flux, load torque, mechanical speed, electromagnetic torque, and stator current from EKF. It also calculates additional indicators, including input power, speed error, and torque variation.

The rotor flux magnitude, stator current magnitude, and speed error are calculated as:

$$|\hat{\Psi}_{r,k}| = \sqrt{\hat{\Psi}_{r\alpha,k}^2 + \hat{\Psi}_{r\beta,k}^2} \tag{25}$$

$$|\hat{\imath}_{s,k}| = \sqrt{\hat{\imath}_{s\alpha,k}^2 + \hat{\imath}_{s\beta,k}^2}, \qquad e_{\omega,k} = \omega_{ref.k} - \hat{\omega}_{m,k}$$

The three phase input power is calculated from the stationary reference frame quantities:

$$P_{in,k} = \frac{3}{2}(u_{s\alpha,k} i_{s\alpha,k} + u_{s\beta,k} i_{s\beta,k}) \tag{26}$$

Since instantaneous estimated values may contain small fluctuations, the quantities used by the supervisor are smoothed before the feedback decision is made. For a general variable z_k, exponential smoothing is expressed as

$$\bar{z}_k = \lambda z_k + (1 - \lambda)\bar{z}_{k-1} \qquad 0<\lambda\leq 1 \tag{27}$$

The supervisor compares the smoothed estimated quantities with predefined operating ranges. When the estimated rotor flux decreases under a significant mechanical load, the application calculates a gradual adjustment to an inverter compensation parameter related to the voltage to frequency characteristic. When the estimated operating condition returns to an acceptable range, the command is maintained or adjusted in the opposite direction.

The supervisory rule $g(\cdot)$ is implemented using predefined operating thresholds. When the smoothed rotor flux falls below its acceptable range, the estimated load torque is significant, and the speed error indicates a reduction in motor speed, the rule generates a positive adjustment to increase the inverter compensation parameter. When the rotor flux returns to the acceptable range, the current command is maintained. If the estimated flux approaches its upper operating limit, the rule maintains or gradually reduces the inverter compensation parameter to prevent excessive excitation.

The command variation is limited to prevent a sudden change in inverter operation, while the final parameter value is restricted to an admissible range:

$$\Delta P_{r,k} = sat[g(|\bar{\Psi}_{r,k}|, |\bar{T}_{L,k}|, \bar{P}_{in,k}, e_{\omega,k}), \Delta P_{min}, \Delta P_{max}] \quad (28)$$

$$P_{r,k} = sat(P_{r,k-1} + \Delta P_{r,k}, P_{r,min}, P_{r,max}) \quad (29)$$

Here, $g(\cdot)$ represents the threshold based supervisory rule that assigns a positive, zero, or negative command variation according to the estimated rotor flux, load torque, input power, and speed error. $\Delta P_{r,k}$ is the calculated command variation, while $P_{r,k}$ is the updated inverter parameter. The saturation functions restrict both the command variation and the final parameter value to predefined safe limits.

After calculation, the command is converted into the numerical format required by the inverter register and transmitted through Modbus TCP. A new value is sent only when it differs from the command currently applied to the inverter, avoiding unnecessary communication and repeated register updates.

Two operating modes are considered. When the communication path from the virtual representation to the inverter is disabled, measurements are transferred only from the physical system to the virtual model. In this mode, the implementation operates as a Digital Shadow. When feedback is enabled, the estimated states are evaluated, and a limited control command is returned to the inverter. This bidirectional exchange of information corresponds to Digital Twin operation.

The seven methodological steps therefore establish a complete workflow from physical operation and measurement to virtual state estimation and feedback intervention. The same experimental platform can therefore function either as a monitoring system or as a Digital Twin with feedback capability.

3 Results

3.1 Experimental Conditions

The experiments were conducted at inverter reference frequencies of 40 Hz and 45 Hz. Two operating modes were compared. In Digital Shadow mode, the virtual model was synchronized with the physical drive without modifying the inverter parameter. In Digital Twin mode, the estimated states were additionally used to generate feedback command for the inverter.

3.2 Online State Estimation

Fig 2 and Fig 3 compare the rotor speed measured by the incremental encoder with the speed estimated by the EKF. In both operating modes, the estimated speed follows the measured response during startup, operation at 40 Hz, and the transition to 45 Hz. This agreement indicates that the EKF remains synchronized with the mechanical behavior of the physical drive.

In Digital Shadow mode, the speed gradually decreases at 40 Hz because the motor is unable to sustain the applied mechanical load under the existing inverter setting. When the reference frequency is increased to 45 Hz, the motor accelerates again and reaches a higher stable speed.

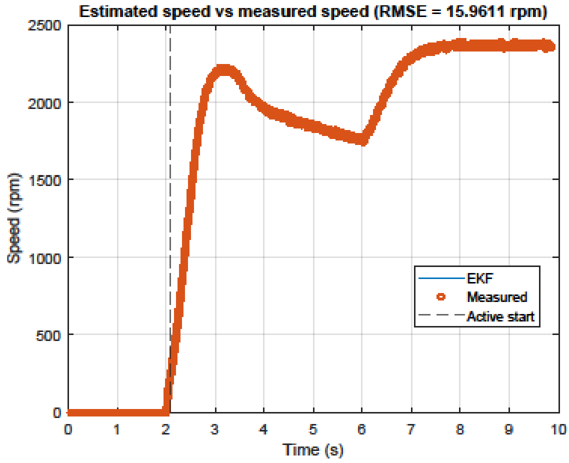

Fig 2_Measured and EKF estimated rotor speed during Digital Shadow operation, showing close estimator tracking and a gradual speed reduction at 40 Hz.

In Digital Twin mode, the speed reduction at 40 Hz is less evident and the motor operates more steadily. Since the same model and EKF are used in both tests, this improvement is attributed to the feedback command applied to the inverter.

3.3 Rotor Flux and Feedback Effect

Fig 4 and Fig 5 present the estimated rotor flux components and magnitude for the two operating modes. In Digital Shadow mode, the estimated flux increases after startup but subsequently decreases during operation at 40 Hz. This reduction in magnetization is accompanied by a gradual decrease in motor speed. Because the feedback path is disabled, the virtual system can identify this condition but cannot modify the physical operation of the drive.

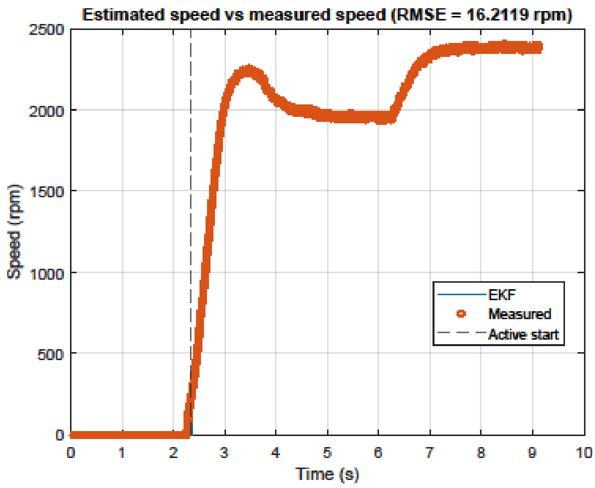

Fig 3_Measured and EKF estimated rotor speed during Digital Twin operation, showing close estimator tracking and improved speed stability at 40 Hz under feedback control.

In Digital Twin mode, the estimated rotor flux and mechanical load information are evaluated by the supervisory application. When insufficient flux is detected under load, the inverter parameter affecting the voltage to frequency characteristic is adjusted gradually. The returned command improves flux retention and supports more stable motor operation at 40 Hz.

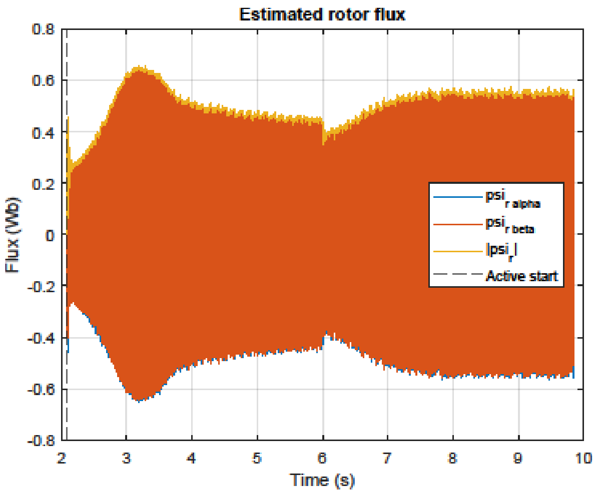

Fig 4_ Estimated rotor flux components and magnitude during Digital Shadow operation, showing a gradual reduction in rotor flux at 40 Hz without inverter feedback.

The comparison therefore demonstrates the functional difference between the two modes. The Digital Shadow provides online monitoring and synchronization of the virtual model with the physical drive, whereas the Digital Twin additionally uses the estimated states to influence the subsequent operation of the motor.

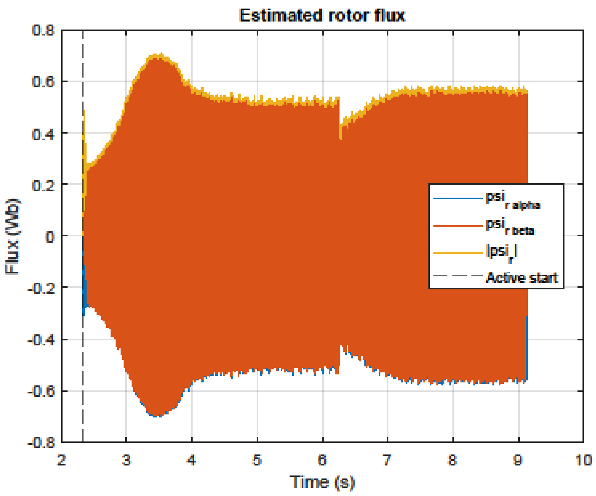

Fig 5_Estimated rotor flux components and magnitude during Digital Twin operation, showing improved rotor flux retention after adjustment of the inverter compensation parameter.

Table 4. Quantitative comparison at 40 Hz

Metric	Digital Shadow	Digital Twin	Difference
Speed estimation RMSE	15.96 rpm	16.21 rpm	Comparable accuracy
Speed near the end of the 40 Hz interval	approximately 1760 rpm	approximately 1960 rpm	approximately 11% higher
Mean rotor flux (4.0–5.9 s)	approximately 0.475 Wb	approximately 0.535 Wb	approximately 13% higher

To quantify the differences between the two operating modes, the speed and rotor flux curves were compared during operation at 40 Hz. The speed estimation RMSE was 15.96 rpm in Digital Shadow mode and 16.21 rpm in Digital Twin mode, showing similar estimation accuracy. However, Digital Twin operation maintained approximately 11% higher rotor speed near the end of the 40 Hz interval The mean estimated rotor flux magnitude was also approximately 13% higher than in Digital Shadow mode.

3.4 Discussion

The results show that EKF can follow changes in the motor operating state during startup and transitions between reference frequencies. The speed comparison validates the online estimation process, while the rotor flux results demonstrate the effect of the returned inverter command.

The speed reduction observed in Digital Shadow mode at 40 Hz is consistent with insufficient voltage compensation under mechanical load. At the lower operating frequency, the stator voltage drop becomes more significant relative to the applied voltage, reducing the effective air gap flux and the available electromagnetic torque. Consequently, the motor develops insufficient torque to maintain its initial speed, resulting in gradual speed reduction. In Digital Twin mode, the supervisory application detects the decrease in estimated rotor flux together with the load and speed error and gradually increases the inverter compensation parameter. This adjustment raises the applied voltage at the same frequency, improves rotor flux and torque production, and therefore reduces the speed decrease while avoiding excessive excitation through predefined command limits.

These results demonstrate that the feedback system improves flux retention and motor stability, supporting its classification as a Digital Twin rather than only as a Digital Shadow.

3.5 Limitation

Limitations of the current study include: (i) the framework works in soft real-time on a standard PC, meaning that precise timing cannot be guaranteed; (ii) the experimental verification of the proposed model was carried out on a single induction motor with a particular loading condition; (iii) the accuracy of the EKF depends on the identified motor parameters, making it sensitive to variations in these parameters; and (iv) the EKF was not compared with other state observers; therefore, its relative performance should be evaluated against alternative methods.

4 Conclusion

This paper presented an experimental Digital Twin framework for an induction motor drive, integrating measurement acquisition, signal processing, a nonlinear virtual model, online state estimation, and feedback communication with the inverter. The EKF successfully synchronized the virtual model with physical drive and accurately followed the measured rotor speed under changing operating conditions.

The comparison between Digital Shadow and Digital Twin operation demonstrated the importance of the feedback path. Without feedback, the motor was unable to continuously sustain the applied load at 40 Hz, leading to reduced rotor flux and a gradual decrease in speed. In Digital Twin mode, the estimated states were used to adjust the inverter operation, improving flux retention and supporting more stable motor behavior. The results confirm that the proposed implementation provides both online monitoring and bidirectional interaction with the physical drive.

Future work will focus on implementing the proposed framework on a deterministic real time platform to improve computational performance. The system will also be evaluated under a range of operating frequencies, load levels, and transient conditions. Further research will develop estimation and supervisory methods to reduce sensitivity to motor parameter variations and measurement disturbances. In addition, the framework will be extended to support more advanced monitoring and control functions for induction motor drives.

References:

1. D. Dhamo, A. Spahiu, and D. Panxhi, “Digital twins in electric drives: A review and proposed framework,” *Power Electronics and Drives*, vol. 11, no. 1, pp. 299–315, 2026, doi: 10.2478/pead-2026-0021.
2. W. Kritzinger, M. Karner, G. Traar, J. Henjes, and W. Sihn, “Digital Twin in manufacturing: A categorical literature review and classification,” IFAC-PapersOnLine, vol. 51, no. 11, pp. 1016–1022, 2018.
3. F. Tao, J. Cheng, Q. Qi, M. Zhang, H. Zhang, and F. Sui, “Digital twin-driven product design, manufacturing and service with big data,” Int. J. Adv. Manuf. Technol., vol. 94, pp. 3563–3576, 2018.
4. T. H.-J. Uhlemann, C. Lehmann, and R. Steinhilper, “The Digital Twin: Realizing the cyber-physical production system for Industry 4.0,” Procedia Manuf., vol. 11, pp. 335–340, 2017.
5. Y. Lu, C. Liu, K. I.-K. Wang, H. Huang, and X. Xu, “Digital Twin-driven smart manufacturing: Connotation, reference model, applications and research issues,” Robot. Comput.-Integr. Manuf., vol. 61, Art. no. 101837, 2020.
6. D. Simon, Optimal State Estimation: Kalman, H∞, and Nonlinear Approaches. Hoboken, NJ, USA: Wiley, 2006.
7. P. Vas, Sensorless Vector and Direct Torque Control. Oxford, U.K.: Oxford Univ. Press, 1998.
8. M. Barut, S. Bogosyan, and M. Gokasan, “Speed-sensorless estimation for induction motors using extended Kalman filters,” IEEE Trans. Ind. Electron., vol. 54, no. 1, pp. 272–280, 2007.
9. E. Zerdali and M. Barut, “The comparisons of optimized extended Kalman filters for speed-sensorless control of induction motors,” Power Electron. Drives, vol. 3, no. 1, pp. 25–44, 2018.
10. R. Babau, I. Boldea, T. J. E. Miller, and N. Muntean, “Complete parameter identification of large induction machines from no-load acceleration-deceleration tests,” IEEE Trans. Ind. Electron., vol. 54, no. 4, pp. 1962–1972, 2007.
11. D. Lindenmeyer, H. W. Dommel, A. Moshref, and P. Kundur, “An induction motor parameter estimation method,” Int. J. Electr. Power Energy Syst., vol. 23, no. 4, pp. 251–262, 2001.
12. Y. Koubaa, “Application of least-squares techniques for induction motor parameters estimation,” Math. Comput. Model. Dyn. Syst., vol. 12, no. 4, pp. 363–375, 2006.
13. V. P. Sakthivel, R. Bhuvaneswari, and S. Subramanian, “Multi-objective parameter estimation of induction motor using particle swarm optimization,” Eng. Appl. Artif. Intell., vol. 23, no. 3, pp. 302–312, 2010.
14. D. Bhowmick and S. K. Chowdhury, “Estimation of induction motor equivalent circuit parameters and losses from transient measurement,” ISA Trans., vol. 157, pp. 573–590, 2025.